Food Control 133 (2022) 108577

Contents lists available at ScienceDirect

Food Control

journal homepage: www.elsevier.com/locate/foodcont

Inactivation efficacies of lactic acid and mild heat treatments against *Escherichia coli* strains in organic broccoli sprouts

Lin Chen [a,b], Qin Liu [a,b], Xue Zhao [a,b], Hongfei Zhang [a], Xinyi Pang [a], Hongshun Yang [a,b,*]

[a] Department of Food Science and Technology, National University of Singapore, 117542, Singapore
[b] National University of Singapore (Suzhou) Research Institute, 377 Lin Quan Street, Suzhou Industrial Park, Suzhou, Jiangsu 215123, PR China

ARTICLE INFO

Keywords:
Organic acid
Mild heat
Modelling
Pathogen
Metabolomics
Vegetable sprout

ABSTRACT

The kinetics of the inactivation of *Escherichia coli* in organic broccoli sprouts by mild heat (MH) and lactic acid (LA) were investigated. *In vitro* survival kinetics showed that the cell number decreased dramatically and was not detectable after 120–135 s under combination treatment. Protein leakage and atomic force microscopy analyses showed that inactivation of *E. coli* cells resulted from disruption of the outer membrane by the sanitisers. LA almost destroyed the outer membrane and induced high protein leakage (3.78–10.75 μg/mL). MH enhanced the membrane damage caused by LA. The *in vivo* inactivation and following recovery during storage suggested that the combination treatment presented a potential inactivation process for organic vegetables or sprouts. Weibull model with higher R^2 values (0.66–0.99) best described the *in vitro* antibacterial kinetics and *in vivo* recovery dynamics. Moreover, the metabolic analysis revealed that citrate cycle (TCA) and amino acid metabolism contributed to the adaptive responses.

1. Introduction

The consumption of fresh organic sprouts has dramatically increased in recent decades due to the increased consumer awareness of their nutritive values. Epidemiological studies revealed that the risks of some chronic diseases and cancers correlate negatively with the consumption of certain sprout produce (Chen, Zhang, et al., 2019). However, more foodborne outbreaks associated with fresh organic sprouts have been reported in recent years, in parallel with increases in organic sprouts production and consumption. Pathogens, such as *Escherichia coli* O157:H7, *Salmonella enterica*, and *Listeria monocytogenes*, are responsible for these foodborne infections (Harvey et al., 2016). From 1992 to 2014, 18 outbreaks from organic foods (e.g., sprouts produce) were documented, resulting in 779 illnesses, 258 hospitalizations, and 3 deaths (Ferelli & Micallef, 2019). Organic fruit and vegetables are even more susceptible to fecal contamination because of the limited application of chemical sanitisers (Mukherjee et al., 2004). Therefore, suitable sanitising approaches for organic sprouts should be identified and applied.

Sanitisers, such as sodium hypochlorite, hydrogen peroxide, organic acids, and peroxyacetic acid, are widely used to disinfect fruit and vegetables because of their low cost and effectiveness (Sethi et al., 2020; Pangloli & Hung, 2013). Nevertheless, strict regulations established by the United States Department of Agriculture National Organic Program (USDA NOP) limit the categories and dosages of sanitisers that can be used during the processing and production of organic fruit and vegetables (NOP, 2011). The NOP clarifies that the residual chlorine in water contacted with organic fruit and vegetables should be lower than 4 mg/l. Therefore, alternative disinfectants that meet the organic processing standards should be developed.

Organic acids and their salts are weak acids and have been used in the food industry as additives for years. For instance, acetic acid, lactic acid (LA), and citric acid, are used to improve the specific volume of bread (Su et al., 2019). Moreover, these acids are applied as preservatives of meat products (Ben Braïek & Smaoui, 2021). In addition, the sanitisation effect of organic acids on fresh fruit and vegetables has been widely studied (Yoon & Lee, 2018). For example, soak treatments with lactic (5%, v/v) and acetic acids (5%, v/v) resulted in reductions in the numbers of *E. coli* O157:H7 inoculated in alfalfa seeds by 3.0 and 2.4 log CFU/g, respectively, before sprouting (Lang et al., 2000). Furthermore, LA is Generally Recognised as Safe (GRAS) and its application for organic sprouts is approved by the NOP (2011). Thus, it could be a potential disinfection method for fresh sprouted produce.

Moreover, it has been reported that the physical method mild heat (MH, 40–50 °C) effectively enhanced the antibacterial effects of

* Corresponding author. Department of Food Science and Technology National University of Singapore, 117542, Singapore.
E-mail address: fstynghs@nus.edu.sg (H. Yang).

https://doi.org/10.1016/j.foodcont.2021.108577
Received 22 June 2021; Received in revised form 1 September 2021; Accepted 24 September 2021
Available online 27 September 2021

sanitisers (e.g., LA, citric acid, hydrogen peroxide) on baby spinach (Huang & Chen, 2011). Therefore, the combination treatment of LA and MH was tested in this study. The gram-negative *E. coli* O157:H7, a foodborne pathogenic bacterium, may cause the urinary tract infection, coleocystitis, or septicaemia. *E. coli* O157:H7 was one of the leading causes of outbreaks related to sprouts produce from 2004 to 2012 (Callejón et al., 2015). In addition, in 1996, the largest outbreak related to sprouts consumption occurred in Japan. About 12,000 patients were infected after consuming radish sprouts contaminated with *E. coli* O157:H7. Among the patients, 121 hemolytic uremic syndrome and 12 death cases were recorded (Choi et al., 2016). *E. coli* ATCC 25922 is a subspecies of *E. coli* that is often used as a surrogate species for pathogenic *E. coli* species in food microbiology studies (Lu et al., 2010). Recent studies showed that the strain *E. coli* ATCC 25922 were not suitable to use as a surrogate in some antibacterial tests. For instance, the sanitising effects of LA on *E. coli* strain ATCC 25922 and pathogenic O26:H11 were significantly different (Chen et al., 2020). Therefore, the sanitising effects of LA and MH on the two *E. coli* strains (ATCC 25922 and O157:H7) should be compared.

In this study, the inactivation effects of *E. coli* ATCC 25922 and O157:H7 inoculated in organic broccoli sprouts by LA (2%, v/v), MH (45 °C), and their combination treatment were compared. The *in vitro* inactivation curves of *E. coli* under different treatments were studied and further fitted using five models. The amount of leaked protein and cell morphology changes were further tested. The kinetics of *in vivo* growth recovery of *E. coli* in broccoli sprouts after sanitising treatments were also monitored during storage for 6 d. Lastly, the metabolic responses of the pathogenic *E. coli* O157:H7, which presented higher stress tolerances under different treatments compared with those in ATCC25922, were studied by nuclear magnetic resonance (NMR).

2. Materials and methods

2.1. In vitro inactivation kinetics of E. coli strains

Non-pathogenic *E. coli* (NPE) strain ATCC 25922 and pathogenic *E. coli* (PE) strain O157:H7 (ATCC 35150) were obtained from the Department of Food Science and Technology, National University of Singapore. The strains were cultured in Tryptone Soya Broth (TSB, Oxoid, Basingstoke, UK) for ~12 h at 37 °C. They were then adapted to nalidixic acid (Sigma-Aldrich, St. Louis, MO, USA) in TSB from 20 to 100 μg/mL by rounds of transfers. Overnight cultures of *E. coli* strains were inoculated 1:100 (v/v) in fresh TSB (400 mL) and incubated for 18 h (37 °C) to prepare working suspensions. The bacterial counts were calculated on Tryptone Soya Agar (TSA, Oxoid, Basingstoke, UK). The obtained *E. coli* culture (around 8–9 log colony forming units (CFU)/mL) was centrifuged at 6000×*g* for 10 min (24 °C) and the bacterial pellet was washed three times using phosphate-buffered saline (PBS, pH 7.2).

The microbial suspension was concentrated by resuspending the pellet in 2 mL of sterile saline (8.5 g/l NaCl, pH 7.0) and then well mixed with 8 mL sterile saline (control group, room temperature, 24 ± 1 °C), sterile saline (45 °C), LA (2%, v/v, room temperature) in sterile saline, and the warmed LA solution (45 °C), separately, in 50 mL test tubes. For the MH treatment, the microbial suspension was mixed with pre-warmed solutions (45 °C) and the mixtures were immediately incubated in water bath at 45 °C. During the inactivation process, 1 mL of the mixed suspension was mixed with 9 mL neutralising buffer (0.1 mol/l PBS, pH 7.5, 24 ± 1 °C) every 15 s until 180 s. The neutralised solutions were serially diluted, spread on TSA, and incubated for 48 h at 37 °C. The colonies counts were recorded and expressed as log CFU/mL. The limit of detection was 2 log CFU/mL.

2.2. Mathematical fitting of the antibacterial kinetics

The bacterial reduction points (except points at 90 s Which were used for model verification) of the three sanitising treatments were fitted mathematically using five models (Linear, Weibull, Gompertz, reduced Huang, and reduced Baranyi) in MATLAB R2013b (The Mathworks Inc., Natick, MA, USA) (Ghate et al., 2017).

Linear model: $\log_{10}(y_0/y) = ax + b$, where y_0 is the initial bacterial count, y is the surviving bacterial count, x is the time in s, and a and b are the linear regression parameters.

Weibull model: $\log_{10}(y_0/y) = (x/c)^{\alpha}$, where α represents the shape parameter and c is the time needed to reduce 1 log CFU/mL.

Gompertz model: $\log_{10}(y_0/y) = y_{max}\exp\{-\exp[(\beta e)(\gamma\text{-}x)/y_{max}+1]\}$, where y_{max} is the sanitising effect (log CFU/mL) of each treatment after the maximum treatment time (*In vitro* study: 180 s for MH treatments, 150 s for PE-LA, 135 s for NPE-LA and PE-combination, and 120 s for NPE-combination; *In vivo* study: 6 d for 6 groups). β is the maximum rate of the inactivation kinetics and γ is the lag phase duration.

Reduced Huang model: $\log_{10}(y_0/y) = \beta_1\{x+(1/4)\ln[(1+e^{-4(x-\gamma 1)})/(1+e^{4\gamma 1})]\}$, where β_1 is the maximum antibacterial rate and γ_1 represents lag phase duration in s.

Reduced Baranyi model: $\log_{10}(y_0/y) = \beta_2 x + \ln[\exp(-\beta_2 x)+\exp(-h_0)-\exp(-\beta_2 x-h_0)]$, where x is the treatment time in s, y is the surviving bacterial count, y_0 is the initial bacterial count, β_2 is the maximum antibacterial rate in (log CFU/mL)/s, h_0 is the physiological state (log CFU/mL).

The fitting goodness was examined using R-square (R^2) and root mean squared error (RMSE). Moreover, overfitting was analysed using Akaike information criterion (AIC) values: AIC = nln(SSE) + 2p, where n represents the used data point number, SSE is the sum of squared estimates of error and p is the number of the parameter used.

2.3. Protein leakage

The method described by Liu et al. (2018) was used to test the protein leakage of *E. coli* during the sanitising treatments. The neutralised suspensions collected in section 2.1 at 0, 15, 30, 60, 120, and 180 s were centrifuged at 6000×*g* for 10 min (24 °C). The obtained supernatant (20 μL) was mixed well with 200 μL Coomassie brilliant blue G-250 solution and incubated at room temperature (24 ± 1 °C) for 5 min. The absorbance of the mixture was then examined at 595 nm using a plate reader (Spectrafluor Plus, Tecan, Durham, NC, USA). Bovine serum albumin solutions with concentrations of 20–100 μg/mL were used as standards ($R^2 > 0.99$).

2.4. Atomic force microscopy (AFM) analysis of morphological alterations

Suspensions of *E. coli* were prepared and treated as described in section 2.1. After inactivation for 2 min, the mixture (10 μL) of each group was pipetted on a mica sheet and then dried by an aurilave. After air-drying in a laminar flow cabinet (4 h), the prepared sheet was scanned using a tabletop (TT)-AFM instrument (AFM workshop, Signal Hill, CA, USA) in 4 h. The resonance and force constants were set at 190 kHz and 45 N/m, respectively. Tapping mode with 0.4 Hz scan rate and 512 scan lines was applied to scan the samples (Chen, Zhang, et al., 2019). The offline software Gwyddion (http://gwyddion.net/) was applied to analyse the obtained images. The morphological parameters of *E. coli* strains, including root-mean-square (RMS) roughness, height, and width, were recorded. The central region on the cell surface (0.2 × 0.2 μm^2) was used to calculate RMS roughness and at least 20 measurements were carried out for each parameter.

2.5. In vivo growth kinetics during storage

Organic broccoli (*Brassica oleracea* var. *italica*) seeds were obtained from a local company in Singapore. The seeds were germinated and sprouted according to our previous method (Chen et al., 2018). After sowing for 7 d, the organic broccoli sprouts were harvested carefully. The inoculation of *E. coli* on organic broccoli sprouts was conducted by

submerging the sprouts in a bacterial suspension (around 7 log CFU/mL) for 5 min. The sprouts were then air-dried in a Class II biosafety cabinet (LA2-4A1, ESCO Technologies, Inc., Hatboro, PA, USA) at room temperature for 30 min. In our preliminary study, broccoli sprouts were soaked in 2% (v/v) LA for 0.5, 1, 2, and 4 min. The results showed that 4 min treatment lead to the discoloration of sprouts. Thus, treatment with LA (2%, v/v) for 2 min was applied as the working condition. The prepared sprouts were soaked in sterile deionised (DI) water (control, room temperature), DI water (45 °C), LA (2%, v/v, room temperature), and the combination treatment (2% LA, 45 °C), respectively, for 2 min. The sprouts were then washed by sterile DI water (room temperature) for 1 min to remove the residual LA and to avoid any subsequent discoloration. After the sanitising treatment, the sprouts (100 g) of each group were stored in clear hinged containers (11.4 cm × 11.4 cm × 7.0 cm, length × width × height) in the dark. The temperature was 4–6 °C, while the relative humidity was ~70%.

The sprouts were sampled before and after sanitising treatments at day 0. In the following storage period (6 d), the treated sprouts were sampled daily at the same time. Serial dilutions of the ground samples were prepared and the dilution (0.1 mL) was pipetted on TSA containing 100 μg/mL nalidixic acid. The TSA plates were incubated for 48 h at 37 °C. The results were expressed as log CFU/g fresh weight (FW). The obtained count reduction points (except points at day 4, which were used for model verification) of *E. coli* during storage were further model fitted as in section 2.2 and the related model parameters were also calculated. The selected model was further verified by comparison of the observed and predicted values (Huang et al., 2011). The reliability was evaluated using the bias factor (B_f) and accuracy factor (A_f):

$$Af = exp\left(\sqrt{\frac{\sum_{i=1}^{n}[ln(\mu predict,\ i) - ln(\mu observe,\ i)]2}{n}}\right)$$

$$Bf = exp\left(\frac{\sum_{i=1}^{n}[ln(\mu predict,\ i) - ln(\mu observe,\ i)]}{n}\right)$$

Where $\mu_{predict}$ is the predicted values calculated from selected model, $\mu_{observe}$ is the observed values recorded from plate count, and n stands for the number of observations.

2.6. Physicochemical measurement

Colour changes in broccoli sprout leaves during storage were tested using a Minolta Colorimeter CM-3500d (Konica Minolta, Tokyo, Japan). The colour values (L*, a*, and b*) were measured for each group. L* represented lightness, a* presented redness/greenness, and b* denoted yellowness/blueness of the samples. Colour difference among the different groups was calculated using the formula: $\Delta E^* = \sqrt{(\Delta L^*)^2 + (\Delta a^*)^2 + (\Delta b^*)^2}$, where ΔE* is the overall colour difference, ΔL* is the difference in lightness between treated group and control group at the same day. Similarly, Δa* and Δb* are the differences in redness/greenness and yellowness/blueness, respectively (Zhao, Chen, et al., 2021). The measurements of each group were independently replicated five times. Firmness (cutting force) of the middle hypocotyl of broccoli sprouts was measured by a texture analyser (TA-XT2i, Stable Micro System, Surrey, UK) equipped with a knife blade (TA-42). The pre-test, test, and post speed were 4, 4, and 4 mm/s, respectively. The maximum peak force was recorded as firmness. The total phenolics content was determined by the method of Chen, Tan, et al. (2019). Fresh sprouts samples (1 g) were mixed with 5 mL methanol containing 1% (v/v) hydrochloric acid, and homogenised in cold mortar and pestle. The homogenates were extracted under dark condition for 30 min and then centrifuged (12,000×*g*) at 4 °C for 10 min. The supernatant was collected and the absorbance was recorded at 280 nm. The phenolics content in samples was calculated by a standard curve of gallic acid and expressed as mg/g FW.

2.7. NMR analysis of intracellular metabolic profiles in E. coli

The intracellular metabolites of strain O157:H7 of four treatment groups were extracted according to our previous study (Chen et al., 2020). The neutralised solution (30 mL) prepared in 2.1 was centrifuged (12,000×*g*, 20 min, 4 °C) and the obtained pellet was mixed with 1 mL methanol-d_4 (Cambridge Isotope Laboratories, Tewksbury, MA, USA) and extracted at −20 °C for 48 h. After that, the mixtures were centrifuged at 12,000×*g* at 4 °C (20 min) to obtain the extracts. Trimethylsilylpropanoic acid (TSP) was mixed with the extract with a final concentration of 1 mM before NMR analysis. The samples were tested by a Bruker DRX-500 NMR spectrometer (Bruker, Rheinstetten, Germany). The ^{1}H spectra were collected by the standard NOESY pulse sequence. The metabolites were assigned based on our previous study (Chen et al., 2020). The resulting spectra of four groups were processed by Mestrenova (Mestreab Research SL, Santiago de Compostela, Spain) to create the binned database for multivariate analysis. Hierarchical cluster analysis and principal component analysis (PCA) were performed to separate the variables. Moreover, the supervised orthogonal partial least squares discriminant analysis (OPLS-DA) was conducted to screen the variable importance in projection (VIP) metabolites of the pairwise groups. Based on the VIP results, the pathway analysis was conducted in MetaboAnalyst 4.0 (http://www.metaboanalyst.ca/). The metabolic pathways were concluded using Kyoto Encyclopedia of Genes and Genomes (KEGG) (https://www.genome.jp/kegg/pathway.html).

2.8. Statistical analysis

Data were statistically analysed by analysis of variance (ANOVA) in SPSS (Version 22.0, IBM, Armonk, NY, USA). Means of different treatment groups were compared by the least significant difference (LSD) method. Furthermore, differences with $P \leq 0.05$ were considered significant.

3. Results and discussion

3.1. In vitro sanitising kinetics of E. coli

The sanitising kinetics of two *E. coli* strains under four treatments are presented in Fig. 1. Bacterial counts in the control groups of two strains were maintained at around 9 log CFU/mL. Individual treatment with MH resulted in slight bacterial reductions. At 180 s, the counts were 0.74 and 0.62 log CFU/mL lower than those in the control groups of NPE and PE, respectively. Interestingly, LA (2%, v/v, room temperature) treatment sharply decreased the populations of NPE and PE to 5.53 and 5.96 log CFU/mL, respectively, after 15 s. Moreover, the NPE count was lower than the limit of detection (2 log CFU/mL) after 135 s treatment, while PE was continuously counted to 150 s. A previous study reported that LA with low concentration (0.5%) exhibited a promising *in vitro* inactivation effect on *E. coli* after 2 h of exposure (Wang et al., 2015). Several factors may contribute to the disinfection effect of weak organic acids: for example, uncoupling of energy production and regulation caused by cytoplasmic acidification in microbial cells; toxic levels of dissociated acid anion that modify the structures or functions of intracellular proteins and DNA; increased permeability of the membrane; and specific effects of the individual acid (Mani-Lopez et al., 2012; Wang et al., 2013). In addition, the results implied that NPE was more susceptible to acid stress compared to PE. PE serotypes evolve additional resistant mechanisms which make them have greater abilities to adapt and survive under acidic environment (King et al., 2010). Therefore, the strain ATCC 25922 may be not a suitable surrogate of pathogenic O157:H7 under lactic acid treatment.

Moreover, fast *E. coli* reductions were observed in the groups of combined treatments. The NPE count continuously decreased from 8.99 to 2.04 log CFU/mL after treatment for 120 s. For PE strain, the count reduced from 9.06 to 2.01 log CFU/mL after 135 s. The combined

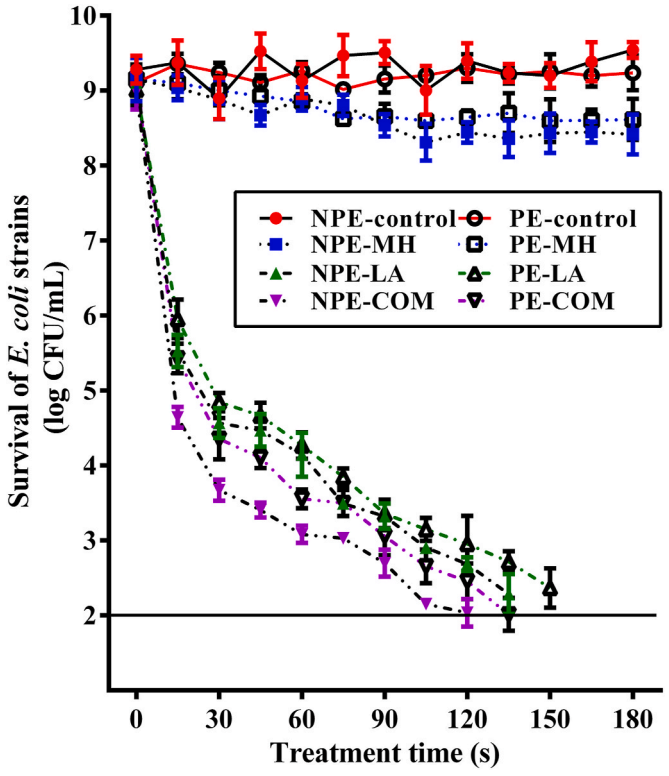

Fig. 1. *In vitro* survival curves of *E. coli* strains (NPE: non-pathogenic *E. coli*; PE: pathogenic *E. coli*) under treatments by mild heat (MH), lactic acid (LA), and their combination.

application of different sanitisers is an effective strategy for pathogen inactivation during food processing. For instance, the combination of electrolysed water with MH, a carvacrol nanoemulsion, or ultrasound effectively enhanced the sanitising effect compared with their individual use (Liu et al., 2020; Sow et al., 2017; Zhao, Li, & Yang, 2021). Our results indicated that the combined use of MH (45 °C) and LA (2%, v/v) exhibited effective *in vitro* inactivation of *E. coli*, and the organic acid contributed the major sanitising effect of combination. Thus, the combination treatment could be a potential processing method for sprouts produce.

3.2. Mathematical fitting of the antibacterial effect

The modelling approach offers the possibility for prediction and simulation of untested scenarios. It is useful for the design of new studies. In addition, model fitting provides a good summarisation and description of the data (Nielsen et al., 2011). Thus, the antibacterial effects of three sanitising treatments were fitted using five models. The fitting curves and related parameters are shown in Fig. S1 and Table 1, respectively. In addition, the parameters of each model are summarised in Table S1. For the MH treatments (NPE and PE), the linear model presented lowest goodness with lower R^2 and relative higher RMSE and AIC values (Table 1). RMSE is generally considered as the most informative goodness index of non-linear and linear fittings, and lower RMSE values indicate better fitness of the model (Scanlon et al., 2015). Moreover, model comparisons can be performed using AIC, which is a robust statistical method. The parameter number and sample size are taken into account, and lower AIC values indicate a better model (Ghate et al., 2017). Furthermore, Weibull and Reduced Baranyi showed good fitness for MH treatment of NPE (Table 1). On the other hand, Weibull and Gompertz are more applicable for the MH (PE) fitting. Thus, Weibull was the best model to describe the MH inactivation kinetics of both NPE

Table 1
Comparison of the model parameters of five models of antibacterial actions and recovery growth kinetics under different treatments.

Treatment	Model	Antibacterial effect				Growth kinetics during storage			
		R^2	RMSE	SSE	AIC	R^2	RMSE	SSE	AIC
MH (NPE)	Linear	0.54^{f}	0.24^{gh}	0.71^{j}	-2.15^{g}	0.51^{hi}	0.29^{f}	0.57^{j}	-2.48^{i}
	Weibull	0.66^{de}	0.22^{h}	0.53^{kl}	-3.65^{h}	0.94^{ab}	0.11^{gh}	0.07^{mn}	-17.09^{l}
	Gompertz	0.68^{de}	0.22^{h}	0.50^{klm}	-2.28^{g}	0.88^{bc}	0.16^{g}	0.13^{lm}	-10.13^{k}
	Reduced Huang	0.65^{e}	0.23^{gh}	0.54^{kl}	-1.33^{f}	0.81^{d}	0.21^{fg}	0.22^{l}	-5.95^{j}
	Reduced Baranyi	0.64^{e}	0.22^{h}	0.55^{kl}	-3.17^{gh}	0.74^{e}	0.22^{fg}	0.30^{kl}	-5.65^{j}
LA (NPE)	Linear	0.27^{g}	1.70^{b}	25.96^{c}	31.31^{c}	0.20^{k}	0.97^{a}	6.53^{b}	17.01^{b}
	Weibull	0.99^{a}	0.23^{gh}	0.42^{lm}	-6.55^{i}	0.97^{a}	0.16^{g}	0.15^{l}	-11.42^{k}
	Gompertz	0.91^{ab}	0.69^{e}	3.33^{gh}	20.44^{d}	0.72^{ef}	0.55^{de}	1.53^{h}	9.38^{f}
	Reduced Huang	0.76^{cd}	1.10^{d}	8.44^{f}	31.59^{c}	0.31^{j}	-12.50^{k}	2.11^{g}	11.99^{de}
	Reduced Baranyi	0.99^{a}	0.22^{h}	0.39^{lm}	-7.21^{i}	0.55^{h}	0.64^{c}	2.45^{ef}	11.15^{e}
Combination (NPE)	Linear	0.01^{i}	2.12^{a}	35.94^{a}	30.65^{c}	0.06^{l}	1.08^{a}	8.17^{a}	18.81^{a}
	Weibull	0.99^{a}	0.20^{h}	0.27^{n}	-11.84^{j}	0.94^{ab}	0.27^{fg}	0.43^{jk}	-2.79^{i}
	Gompertz	0.94^{ab}	0.60^{f}	2.19^{i}	15.42^{e}	0.84^{cd}	-1.25^{i}	2.25^{fg}	12.47^{cd}
	Reduced Huang	0.67^{de}	1.42^{c}	12.13^{d}	35.95^{a}	0.65^{fg}	0.73^{b}	2.69^{def}	13.92^{c}
	Reduced Baranyi	0.99^{a}	0.20^{h}	0.27^{n}	-11.88^{j}	0.63^{fg}	0.69^{bc}	2.82^{d}	12.29^{cd}
MH (PE)	Linear	0.64^{e}	0.12^{i}	0.17^{np}	-18.94^{k}	0.88^{bc}	0.10^{h}	0.07^{mn}	-19.33^{lm}
	Weibull	0.87^{ab}	0.08^{ij}	0.06^{q}	-28.87^{m}	0.93^{ab}	0.08^{h}	0.04^{n}	-21.36^{m}
	Gompertz	0.89^{ab}	0.07^{j}	0.05^{q}	-29.39^{m}	0.94^{ab}	0.09^{h}	0.04^{n}	-20.05^{m}
	Reduced Huang	0.82^{bc}	0.09^{ij}	0.09^{q}	-23.52^{l}	0.94^{ab}	0.08^{h}	0.04^{n}	-20.72^{m}
	Reduced Baranyi	0.78^{cd}	0.10^{ij}	0.11^{pq}	-22.70^{kl}	0.91^{bc}	0.10^{h}	0.06^{mn}	-19.17^{lm}
LA (PE)	Linear	0.13^{h}	1.64^{bc}	26.82^{c}	34.89^{ab}	0.16^{k}	0.78^{b}	4.26^{c}	13.60^{c}
	Weibull	0.98^{a}	0.27^{gh}	0.64^{jk}	-1.27^{f}	0.96^{a}	0.16^{g}	0.15^{l}	-10.97^{k}
	Gompertz	0.89^{ab}	0.67^{e}	3.55^{g}	21.20^{d}	0.70^{ef}	0.47^{e}	1.10^{i}	6.73^{h}
	Reduced Huang	0.73^{de}	1.03^{d}	8.51^{ef}	31.70^{c}	0.62^{gh}	0.53^{de}	1.39^{h}	8.63^{g}
	Reduced Baranyi	0.98^{a}	0.26^{gh}	0.61^{jk}	-1.87^{f}	0.46^{i}	0.57^{d}	1.98^{g}	9.46^{f}
Combination (PE)	Linear	0.09^{i}	1.86^{ab}	31.10^{b}	32.93^{bc}	0.15^{k}	0.95^{a}	6.28^{b}	16.70^{b}
	Weibull	0.98^{a}	0.31^{g}	0.75^{j}	0.53^{e}	0.97^{a}	0.17^{g}	0.18^{l}	-9.71^{k}
	Gompertz	0.91^{ab}	0.66^{ef}	3.06^{h}	19.41^{d}	0.74^{e}	0.49^{e}	1.44^{h}	8.94^{fg}
	Reduced Huang	0.68^{de}	1.25^{cd}	11.00^{de}	34.77^{ab}	0.31^{j}	-11.04^{j}	2.07^{g}	11.81^{de}
	Reduced Baranyi	0.98^{a}	0.30^{g}	0.73^{j}	0.26^{e}	0.57^{h}	0.63^{cd}	2.35^{f}	10.82^{ef}

Note: regression coefficient (R^2), root mean squared error (RMSE), sum of squares for error (SSE) and Akaike information criterion (AIC). LA, lactic acid; MH, mild heat; NPE: non-pathogenic *E. coli*; PE: pathogenic *E. coli*. Within the same column, mean values with different lower cases letters are significantly different from each other ($P \leq 0.05$).

and PE. For the LA treatments, the models of Weibull and reduced Baranyi exhibited good fitness, with high R^2 values of 0.99 and 0.98 for NPE and PE, respectively (Table 1). The low RMSE and AIC values further confirmed that these two models were more applicable for curve fitting of the LA treatments (NPE and PE).

Similarly, the two models also exhibited the best fitting performance for the combined treatment, with higher R^2 and lower RMSE and AIC values (Table 1). Thus, we concluded that the Weibull and reduced Baranyi models were superior models to describe the *in vitro* inactivation kinetics of two *E. coli* under LA and combination treatments. Moreover, the parameters of the Weibull and reduced Baranyi models could provide more information about the inactivation process. For example, Weibull parameter b represents the time needed to reduce 1 log CFU/mL and α indicates the shape characteristic (Ghate et al., 2017). The time (b) needed to reduce 1 log CFU/mL NPE was 0.01 s by combination treatment (Table S1). However, it took longer time (0.04 s) for PE sanitisation. Shape parameters (α) of six groups were all less than 1, indicating concave-downward inactivation curves (Koyama et al., 2017; Luo & Oh, 2016). Furthermore, compared with those in the LA groups, lower physiological state parameters (h_0) in combined treatments were recorded for NPE (−6.59 log CFU/mL) and PE (−5.92 log CFU/mL). The physiological state (h_0) is the product of the maximum inactivation rate and lag (Baranyi & Roberts, 1995). The results indicated greater disinfection effect of the combined treatment compared with that of individual LA treatment. In addition, the lower h_0 of NPE compared with PE further confirmed that the PE was more resistant to the combination treatment.

3.3. Protein leakage under different treatments

Sanitiser-mediated membrane damage was assessed using the protein leakage rate. The results showed that the sanitising treatments negatively affected the membrane integrity of *E. coli* by different degrees (Fig. 2). The concentrations of leaked proteins in the MH groups were similar with those in the control, which remained at a constant and low level (around 2–5 μg/mL). In addition, protein leakage of NPE during LA treatment was improved to 3.56–10.73 μg/mL during *in vitro* inactivation. For PE, LA treatment resulted in lower protein leakage (3.75–7.07 μg/mL) compared with NPE. Complicated mechanisms contribute to the inactivation of *E. coli* under weak acid treatment. Weak acids induce the conversion of unsaturated fatty acids on the membrane into cyclopropane fatty acids, which eventually leads to membrane disruption (Lund et al., 2014). Furthermore, the combined treatment resulted in the highest protein leakage of NPE (20.71 μg/mL) and PE (16.56 μg/mL) after treatment for 180 s. The result indicated that LA is probably the main contributor to the membrane damage caused by the combination treatment and the MH played an auxiliary role.

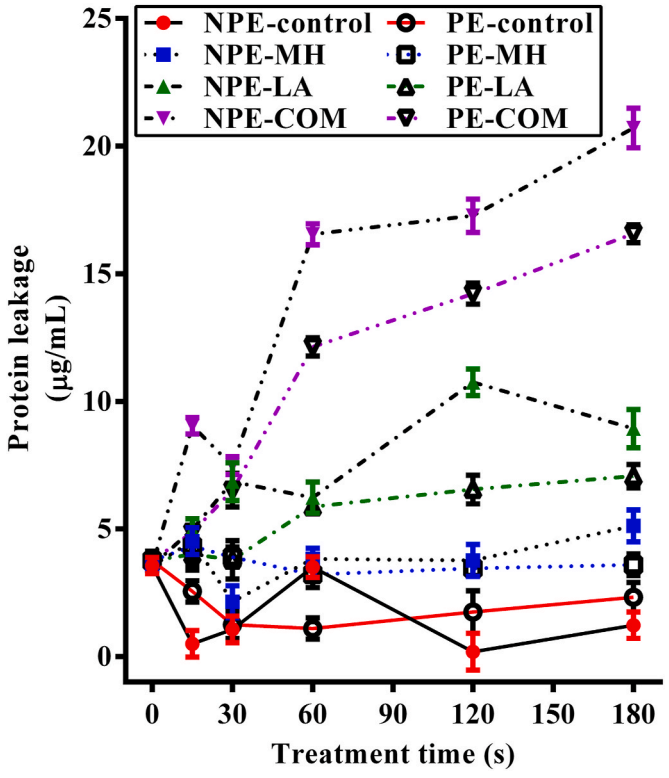

Fig. 2. Effect of different sanitising treatments on the protein leakage from *E. coli* cells. LA, lactic acid; MH, mild heat; NPE: non-pathogenic *E. coli*; PE: pathogenic *E. coli*.

3.4. Morphological changes of E. coli

Atomic force microscopy (AFM) is able to test the 3-dimensional information of cells *in situ* at the nano level. In this study, the morphological changes of *E. coli* under different treatments were tested and are presented in Fig. 3. The images showed that the *E. coli* cells of two serotypes in the control group displayed typical bacilliform morphology with a uniform size. They were aggregated and the cell surface was coarse and irregular (Fig. 3a, e). However, after treatment of MH (45 °C), the cells were inflated and the surface became smoother. Some suspected outer membrane residual components were found on the surface structure (Fig. 3b, f). Similarly, swollen *E. coli* cells with a relative glossy surface were observed under LA treatment (Fig. 3c, g). In addition, the plump cells in combined treatment group also adhered to each other and had full and smooth surfaces (Fig. 3d, h).

Further statistical analysis showed the detailed physical properties (width, height, and roughness) of *E. coli* under each treatment (Fig. 3i). Compared with the cell width (0.85 μm) in the control of NPE, significantly ($P \leq 0.05$) increased cell widths were recorded in the MH (1.08 μm), LA (1.17 μm), and combined treatment (1.34 μm) groups. By contrast, the height of the NPE cells significantly ($P \leq 0.05$) decreased from 0.30 to 0.27, 0.21, and 0.20 μm after sanitising treatments with MH, LA, and their combination, respectively. Moreover, the surface morphology of NPE was analysed quantitatively using the RMS roughness value. The highest roughness value (13.92 nm) was recorded in the control group. The RMS roughness value was reduced to 11.27 nm by MH treatment and to 5.52 nm by LA treatment. The lowest roughness value (2.78 nm) was observed in the combination group. For the PE, similar trends of statistical parameters under four treatments were recorded. PE cells presented highest width (1.37 μm) and lowest height (0.19 μm) and roughness (4.26 nm) in combined treatment group. In addition, the cell surface roughness was significantly ($P \leq 0.05$) higher in PE compared with NPE under LA and combination treatments, indicating the lower rate of membrane disruption of PE group.

Gram-negative *E. coli* is covered by a thick lipopolysaccharide outer membrane, which forms a permeability barrier for environmental stresses such as antibiotics, bacteriophages, and bacteriocins (Putker et al., 2015). The AFM results showed that the sanitising process started with disruption of the outer membrane. After treatment with MH (45 °C), the characteristics of membrane surface were slightly modified, but the cell integrity was still maintained. Membrane permeability might increase because of the structural changes, which was consistent with the results of protein leakage (Wang et al., 2010; Zhang & Hu, 2013). Moreover, LA (2%, v/v) treatment almost destroyed the outer membrane structure and the cytoplasmic membrane was observed to emerge. For gram-negative bacteria, the outer membrane is not a physical barrier to proton movement because the porin diameter is large enough (Lund et al., 2014). In addition to a low pH effect, LA also functions as a permeabiliser of the bacterial outer membrane (Alakomi et al., 2000). Furthermore, the *E. coli* cells collapsed without the support of the outer membrane under the combined treatment. The notable

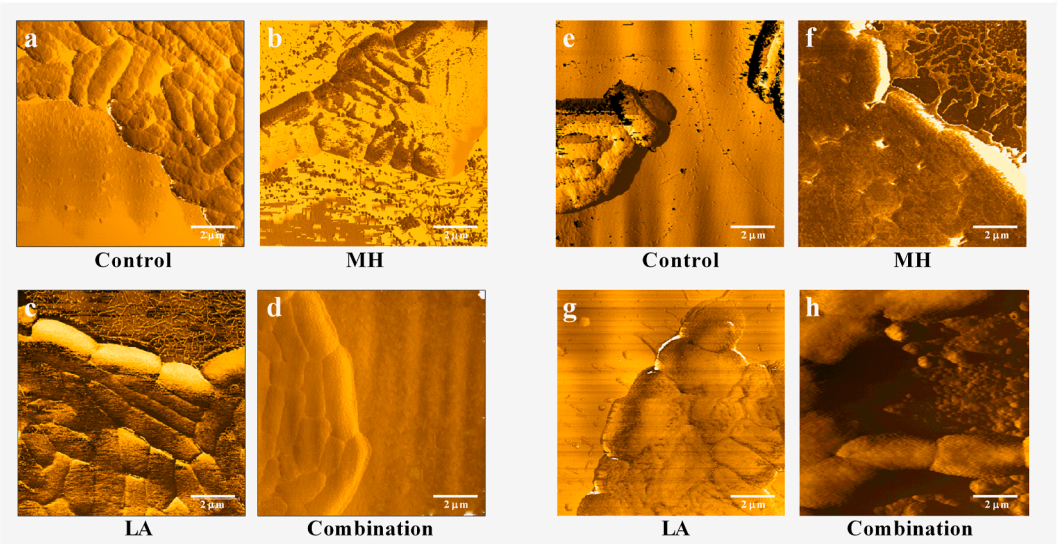

i	NPE				PE			
	Control	MH	LA	Combination	Control	MH	LA	Combination
Width (μm)	0.85^{d}	1.08^{c}	1.17^{b}	1.34^{a}	0.91^{e}	1.15^{bc}	1.25^{ab}	1.37^{a}
Height (μm)	0.30^{a}	0.27^{a}	0.21^{bc}	0.20^{c}	0.28^{a}	0.25^{ab}	0.19^{c}	0.19^{c}
Roughness (nm)	13.92^{a}	11.27^{b}	5.52^{d}	2.78^{f}	13.15^{a}	12.63^{ab}	8.57^{c}	4.26^{e}

Fig. 3. Atomic force microscopy (AFM) images of *E. coli* cells under different disinfectant treatments. Images a-d, NPE cells. Image e-h, PE cells. LA, lactic acid; MH, mild heat; NPE: non-pathogenic *E. coli*; PE: pathogenic *E. coli*.

morphological changes revealed the enhanced disinfectant effect of LA in combination with MH.

3.5. *In vivo* growth kinetics after sanitising treatments

The sanitising effect of each treatment on *E. coli* strains inoculated in broccoli sprouts is shown in Fig. 4. The recovery growth kinetics after disinfectant treatments were monitored during the low temperature (4–6 °C) storage for 6 d. At day 0, the NPE count decreased from 7.12 to 6.73, 5.33, and 5.03 log CFU/g FW after 2 min of MH, LA, and their combination treatment, respectively. For PE, the count was reduced from 7.23 to 6.93, 5.66, and 5.41 log CFU/g FW under MH, LA, and combination treatment, respectively. During storage, populations of *E. coli* cells (NPE and PE) constantly decreased. At day 6, the NPE cell counts were 6.47, 5.98, 4.33, and 3.80 log CFU/g FW in the control, MH, LA, and combination groups, respectively (Fig. 4). Moreover, PE counts in four treated groups at day 6 were 6.56, 6.28, 4.83, and 4.30 log CFU/g FW, respectively. Temperature is a key factor for bacterial growth. It was also observed that *E. coli* did not grow, but survived throughout storage at a low temperature (5 °C) on fresh-cut melon, carrot, and escarole (Abadias et al., 2012). The lower limit of growth for generic *E. coli* is generally believed to be 5 °C (Delaquis et al., 2007). During storage, higher reductions in three treated groups were recorded compared with those in the control groups of both NPE and PE. This might be because the sanitising treatment resulted in a certain proportion of sublethally injured cells that could not survive under long-term low temperature stress (Tian et al., 2018). In addition, it was observed that the inactivation effect of each treatment on *E. coli* (0 d) (Fig. 4) was declined compared with that in the planktonic status (120 s) (Fig. 1). The complex food matrix may weaken the antibacterial effects of the sanitisers (Townsend et al., 2020; Vandekinderen et al., 2009). Nevertheless, the inactivation treatments, especially the combination treatment, exhibited applicable sanitising efficacies.

The model fitting of cell count reduction and related parameters are shown in Fig. S2, Table 1 and Table S2. The results revealed that the Weibull model exhibited best fitness, with higher R^2 values for the three

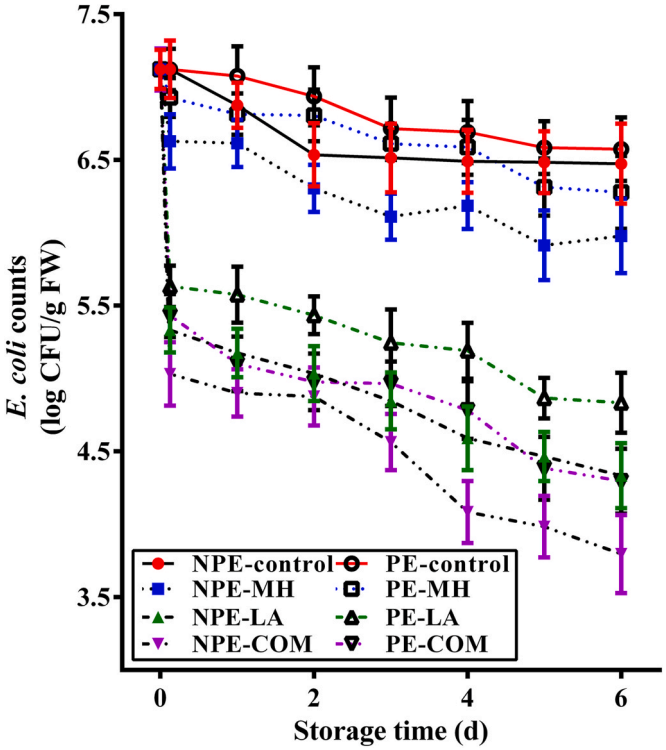

Fig. 4. *In vivo* growth curves of *E. coli* strains (NPE: non-pathogenic *E. coli*; PE: pathogenic *E. coli*) under treatments with mild heat (MH), lactic acid (LA), and their combination.

sanitising groups of two *E. coli* strains. The lowest RMSE, SSE, and AIC values were also recorded (Table 1). Similar to the *in vitro* sanitising kinetics, the LA and combination treatments took significant ($P \leq 0.05$)

less time (0.00 and 0.00 d, respectively) to reduce 1 log CFU/g FW NPE inoculated in sprouts compared with the MH (3.69 d) treatment (Table S2). Furthermore, the sanitisation time of PE by MH (8.20 d) and LA (0.02 d) was significant ($P \leq 0.05$) longer compared that of NPE. Concave-downward cell reduction curves with shape parameters (α) less than 1 were also observed (Fig. S2; Table S2). Thus, we concluded that the Weibull model was applicable to assess the *in vitro* sanitising kinetics and the *in vivo* growth dynamics of *E. coli* under low concentrations of MH, LA, and their combination.

The values predicted by Weibull were compared with the observed values to further verify reliability. The A_f value represents the accuracy of a selected model and B_f is a measurement to estimate the variation between the observed and predicted values. A value of 1 is the ideal result. Table 2 shows that the predicted values of the antibacterial effect curves of NPE and PE at 90 s were close to the observed values. The A_f and B_f values were maintained around 1 (0.87–1.18). Similar results were observed for the *E. coli* count reduction curves during storage. These results verified that the Weibull model was the most suitable strategy to study the sanitising kinetics under each sanitising treatment. The Weibull model is able to illustrate the lag phase or saturation exhibited in an inactivation or growth curve (Ghate et al., 2017; Maresca & Ferrari, 2017). The model showed that lag phases existed in the inactivation (60–180 s) and growth curves (2–6 d) of the three groups (Fig. S1; Fig. S2). Thus, the antibacterial properties of the sanitisers and the compatibility of the Weibull model contributed to the fitting success.

3.6. Physicochemical changes of organic broccoli sprouts

Sprout products are usually stored at low temperature and consumed fresh. The sanitising process should not affect the sprout quality. Thus, the physicochemical changes of the treated sprouts during storage were tested (Table 3). The results indicated that the colour parameters, including L*, a* and b*, in the control group were maintained during storage of 6 d. Moreover, the three sanitising treatments did not significantly ($P \leq 0.05$) change the colour characteristics (L*, a* and b*) compared with those of the control group. Furthermore, the overall colour difference ΔE* remained at a low level in each sanitising group, except for the ΔE* of the MH and LA treatments at day 4.

Texture is another important property to evaluate the commercial value and quality of postharvest produce. In addition, phenolic compounds are important plant compounds and consumed as antioxidants widely (Chen et al., 2018). Our results indicated increasing trends of firmness levels in four groups were observed during 6 days' storage (Table 2). Compared with the firmness results in control (21.09×10^{-2} N), MH (21.22×10^{-2} N), LA (22.31×10^{-2} N) and combined (21.35×10^{-2} N) groups at day 0, they were significantly ($P \leq 0.05$) increased to 25.83, 24.66, 27.11 and 25.88×10^{-2} N, respectively at day 6. Moreover, almost no notable differences of firmnesses among the four groups at each storage day except day 2 (firmness in control group showed significant higher firmness level than those of MH and combination groups). Similarly, McCollum et al. (1993) and Fan et al. (2003) reported slightly decreased firmness in MH treated lettuce and mango fruit, respectively. The mechanism of heat treatment on textural change is not clear. The exposure to MH may result in convertible structural changes of cell wall materials (e.g., pectin) and lead to decrease in firmness (Liu et al., 2017).

Table 3
The physicochemical parameters of organic broccoli sprouts under different antibacterial treatments during 6 days of storage.

Parameter	Treatment	Day 0	Day 2	Day 4	Day 6
L*	Control	31.45^{Aa}	33.12^{Aa}	27.58^{Aa}	31.68^{Aa}
	MH	32.41^{Aa}	32.31^{Aa}	31.25^{Aa}	32.73^{Aa}
	LA	33.63^{Aa}	30.87^{Aa}	29.77^{Aa}	31.10^{Aa}
	Combination	28.65^{Aa}	29.63^{Aa}	27.05^{Aa}	32.20^{Aa}
a*	Control	-8.25^{Aa}	-8.09^{Aa}	-7.40^{Aa}	-7.57^{Aa}
	MH	-8.41^{Aa}	-8.24^{Aa}	-7.21^{Aa}	-7.62^{Aa}
	LA	-8.39^{Ba}	-6.83^{Aa}	-7.87^{ABa}	-8.65^{Ba}
	Combination	-7.31^{Aa}	-7.24^{Aa}	-7.73^{Aa}	-7.92^{Aa}
b*	Control	19.42^{Aa}	20.73^{Aa}	22.67^{Aa}	22.58^{Aa}
	MH	20.31^{Aa}	21.03^{Aa}	24.71^{Aa}	22.07^{Aa}
	LA	20.55^{Aa}	19.74^{Aa}	25.39^{Aa}	25.47^{Aa}
	Combination	20.48^{ABa}	19.61^{Ba}	23.15^{Aa}	21.79^{ABa}
ΔE*	MH	5.23^{Ba}	6.84^{ABa}	10.68^{Aa}	7.11^{ABa}
	LA	5.05^{Ba}	6.58^{ABa}	9.62^{Aa}	7.02^{ABa}
	Combination	3.97^{Aa}	6.50^{Aa}	7.91^{Aa}	4.13^{Aa}
Firmness ($\times 10^{-2}$ N)	Control	21.09^{Ba}	27.06^{Aa}	24.32^{ABa}	25.83^{Aa}
	MH	21.22^{Ba}	22.31^{ABb}	23.15^{ABa}	24.66^{Aa}
	LA	22.31^{Ba}	24.97^{ABab}	25.43^{ABa}	27.11^{Aa}
	Combination	21.35^{Ba}	23.62^{ABb}	23.41^{ABa}	25.88^{Aa}
Total polyphenol content (mg/g FW)	Control	1.25^{Aa}	1.19^{Aa}	1.04^{Aa}	1.02^{Aa}
	MH	1.19^{Aa}	1.21^{Aa}	1.02^{Aa}	1.01^{Aa}
	LA	1.26^{Aa}	1.18^{Aa}	1.05^{Aa}	0.99^{Aa}
	Combination	1.20^{Aa}	1.15^{ABa}	1.11^{ABa}	0.94^{Ba}

Note: Within the same column, mean values of each parameter with different lowercase letters are significantly different from each other ($P \leq 0.05$); within the same row, mean values with different capital letters are significantly different from each other ($P \leq 0.05$). L* represents lightness, a* presents redness/greenness, and b* denotes yellowness/blueness of the samples. LA, lactic acid; MH, mild heat.

For the total phenolics contents in broccoli sprouts, almost no significant changes among the treated groups at each storage day were recorded (Table 3). Furthermore, the total phenolics contents were maintained at levels ranging from 1.02 to 1.25 mg/g FW in control group. Also, relative constant concentrations of total phenolics in MH (1.01–1.21 mg/g FW) and LA (0.99–1.26 mg/g FW) treated groups were presented. For combination treatment, the total phenolics contents were significantly ($P \leq 0.05$) decreased from 1.20 (day 0) to 0.94 mg/g FW (day 6). Generally, the physicochemical properties of broccoli sprouts were not influenced by the MH, LA, or the combination treatments.

3.7. Metabolic profiles of *E. coli* O157:H7 under different sanitising treatments

The pathogenic O157:H7 presented higher stress resistance compared with the NPE. Thus, the metabolic response of the PE was further studied by NMR. The ^{1}H spectra of four groups are shown in Fig. 5. Totally 38 compounds were identified in the extraction samples

Table 2
Accuracy and bias factors of predicted and observed values of *E. coli* counts.

Treatment	*In vitro* antibacterial effect (90 s)				*In vivo* count reduction (4 d)			
	P	O	A_f	B_f	P	O	A_f	B_f
MH (NPE)	0.70^{b}	0.97^{a}	1.18	0.87	1.02^{a}	0.93^{a}	1.10	1.09
LA (NPE)	6.08^{a}	6.18^{a}	1.17	0.90	2.49^{a}	2.53^{a}	1.17	0.96
Combination (NPE)	6.77^{a}	6.81^{a}	1.21	0.96	2.91^{a}	3.04^{a}	1.21	0.88
MH (PE)	0.47^{a}	0.50^{a}	1.03	0.97	0.63^{a}	0.53^{a}	1.11	1.10
LA (PE)	5.50^{a}	5.40^{a}	1.11	1.10	2.03^{a}	1.93^{a}	1.18	1.10
Combination (PE)	6.00^{a}	5.80^{a}	1.07	0.98	2.48^{a}	2.34^{a}	1.17	1.15

Note: Predicted values (P); Observed values (O); Accuracy factors (A_f); Bias factors (B_f). Within the same row in *in vitro* or *in vivo* study, mean values of each parameter with different lowercase letters are significantly different from each other ($P \leq 0.05$). LA, lactic acid; MH, mild heat; NPE: non-pathogenic *E. coli*; PE: pathogenic *E. coli*.

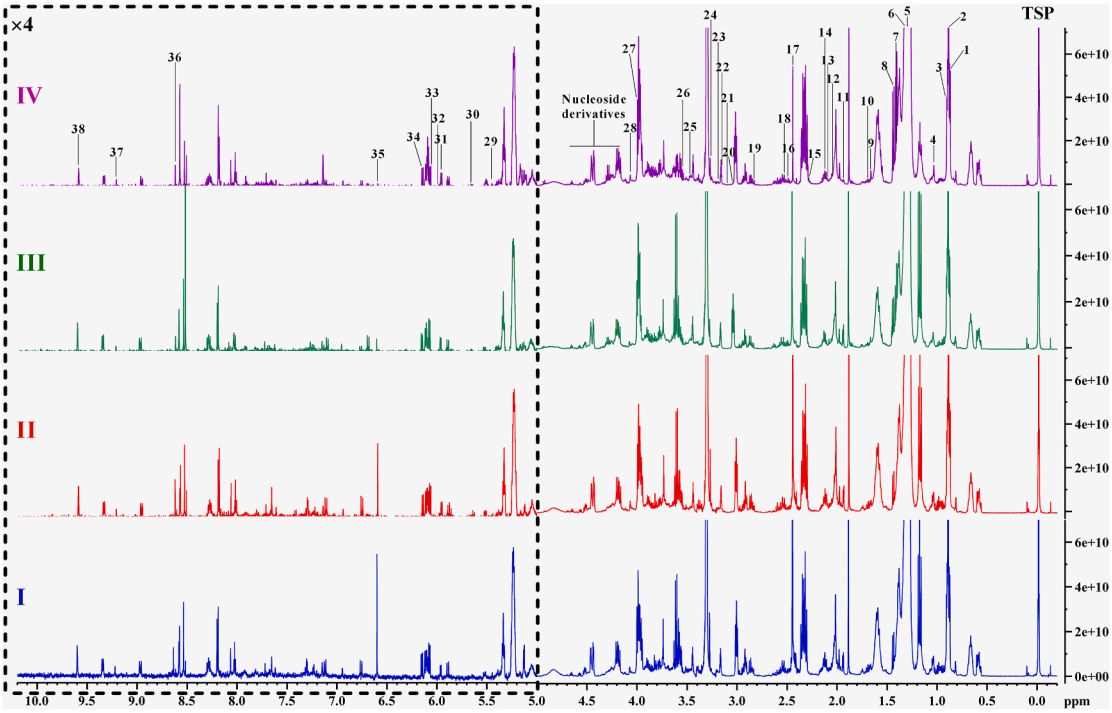

Fig. 5. ^{1}H spectra of pathogenic *E. coli* O157:H7 under different treatments. Note: I, control; II, mild heat (MH) treatment; III, lactic acid (LA) treatment; IV, combination treatment.

(Table S3). Multiple peaks located at 0.5–5 ppm were assigned as sugar and aliphatic acids such as glucose, ribose, acetic acid, and arginine (Chen et al., 2020). Furthermore, other metabolites such as nucleotides were identified in the region of 5–10 ppm. The ^{1}H spectra also presented signal differences among the four groups. For examples, the peak 35 at 6.55 ppm, which was assigned as fumaric acid, showed higher intensities in groups I and II compared with those in III and IV. It indicated that fumaric acid related metabolism may be related with the resistant response to LA stress.

Further hierarchical cluster analysis showed that the four groups of PE were divided into two major clusters: C1 and C2 (Fig. 6a). The subgroup C1 comprised I (control) and II (MH), indicating their metabolic similarities. Moreover, groups III (LA) and IV (combination) were aggregated in C2 and distinguished from the groups I and II. The results indicated that the MH resulted in slight metabolic alteration, while dramatic metabolic response occurred under LA and combination treatments. PCA was conducted to screen the principle metabolites responsible for the variable separation. The first two principle components (PCs) explained the majority of the data (PC1: 48.76%; PC2: 28.83%). The score plot presented the separation of four groups, and the loading plot showed the principle metabolites responsible for the separation (Fig. 6b and c). Group I and II were aggregated, and negatively affected by PC1 and positively affected by PC2. Metabolites such as pyruvic acid were closely related to the two groups. However, group III, which characterised by succinic acid, was negatively related to PC2, indicating the metabolic difference of III compared with I and II. In addition, group IV was separate and positively affected by PC1. Metabolites including threonine, valine, leucine, and lysine were related to group IV.

The OPLS-DA revealed the metabolic discriminations of pairwise groups (I-II; I-III; I-IV) (Fig. 6d–f). The downward peaks in loading S-line presented higher contents of certain metabolites in group I, while peaks pointed upward indicated higher contents in the other groups. Moreover, the significant metabolites with VIP $>$ 1 and $P \leq 0.05$ were highlighted and marked in the S-line. Based on the obtained discriminative metabolites, the pathway analysis was conducted and the results are shown in Fig. 7 and Tables S4–6. The results showed that MH resulted in the increased concentrations of succinic acid and valine. However, some other metabolites such as β-D-glucose, α-ketoglutaric acid, pyruvic acid, and threonine were consumed during the MH response. Generally, 9 metabolic pathways were altered significantly ($P \leq 0.01$) by the MH treatment and citrate cycle (TCA) was the most affected pathway (Fig. 7a; Table S4). Furthermore, the transformation of various amino acids was also monitored. Similar results were recorded in the pairwise groups I-III and I-IV. The results indicated that energy metabolism was related to the stress responses of MH and LA in PE. Indeed, energy production is one of the most important physiological activities of *E. coli* (Orth et al., 2011). It is a crucial feature for *E. coli* to preserve energy status during stringent response and general stress (oxidation, cold, heat, etc.) response (Jozefczuk et al., 2010). Under long-term heat stress (around 2 h), the breakdown and degradation of certain proteins are required for the synthesis of new amino acids such as valine. This process is important for the survival of PE under heat stress. In our study, the short time treatment of MH also resulted similar results.

E. coli have evolved various mechanisms to adapt the acidic stress (Lund et al., 2014). For example, F_1–F_0 ATPase can pump out the intracellular protons actively using energy. Amino acid related decarboxylase/antiporter system also contribute to the survival of *E. coli* under acid environment. In our previous work, PE O26:H11 showed strong acid resistance and the metabolic analysis showed that, besides the higher level of energy production, glutamic acid dependent decarboxylase/antiporter system also played a key role during the acidic adaption (Chen et al., 2020). In this study, lysine content was increased in PE O157:H7 under acid treatment. Therefore, lysine decarboxylase might play an important role in the survival of O157:H7. Moreover, higher level of proline was recorded (Fig. 6e). It is an important energy source and helps protect *E. coli* cells from various biotic and abiotic stress by keeping redox homeostasis and osmolarity (Zhang et al., 2015). Under combination treatment, significant higher contents of amino acids such as lysine, valine, and leucine were detected in O157:H7 (Fig. 6f). However, the TCA related metabolites (fumaric acid, succinic acid, and α-ketoglutaric acid) were dramatically consumed. The

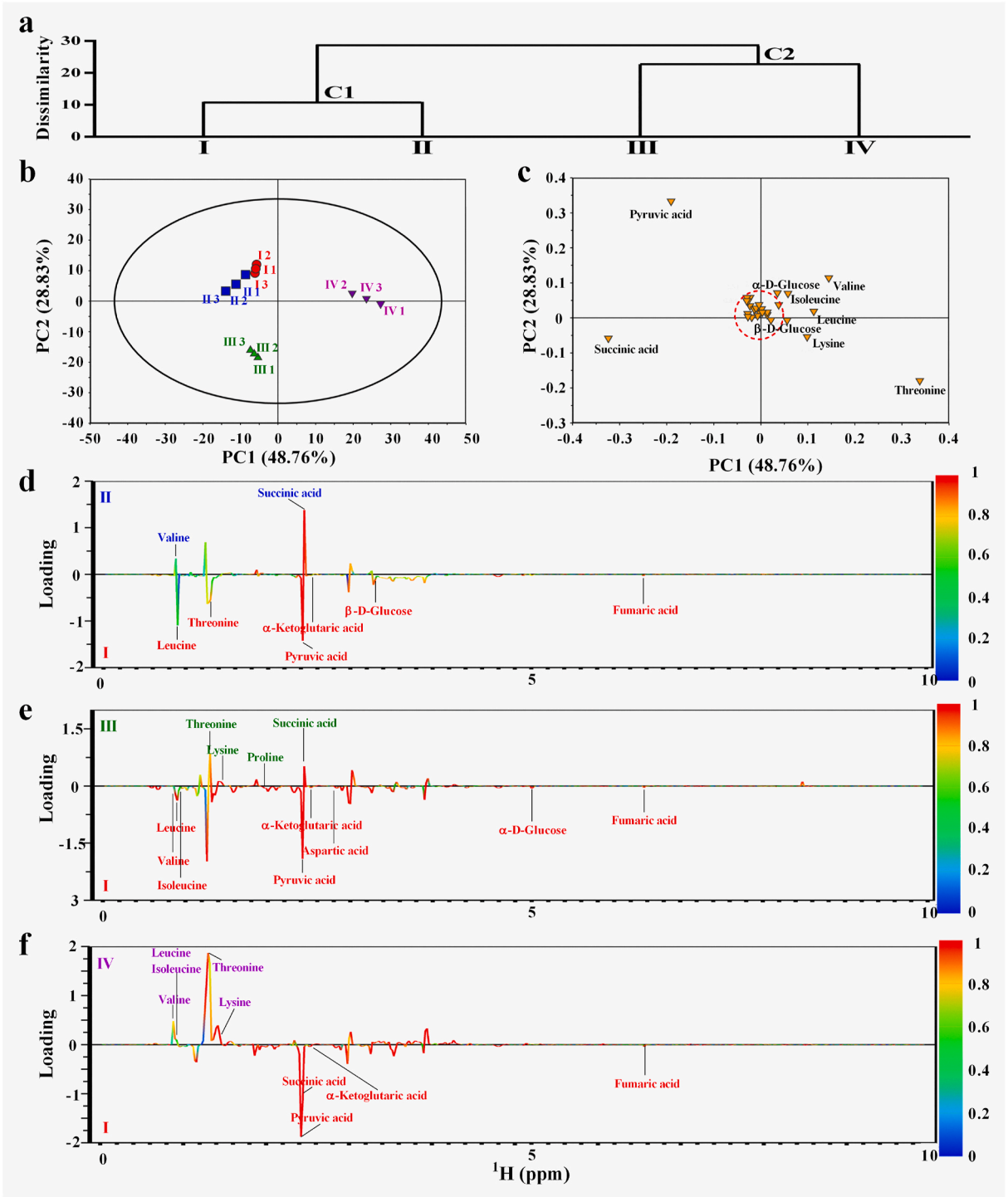

Fig. 6. Hierarchical cluster analysis of four groups (a); score plot of principal component analysis (PCA) (b); loading plot of PCA (c); orthogonal partial least squares discriminant analysis (OPLS-DA) of pairwise groups (d–f). Note: I, control group; II, mild heat treatment; III, lactic acid treatment; IV, combination treatment.

pathway analysis also showed that amino acid synthesis was the most affected pathway (Fig. 7c; Table S6). Based on the VIP, OPLS-DA, pathway analysis, and KEGG database, the hypothesised biochemical pathway of PE O157:H7 under combined treatment was summarised and illustrated in Fig. 7d. The TCA cycle was strongly inhibited which might result from the dramatic consumption of energy for the stress adaption. Moreover, the transformations of amino acids provided energy source and stress adaption related amino acids such as lysine.

4. Conclusion

The inactivation effects of MH (45 °C), LA (2%, v/v), and their combination on two *E. coli* strains were investigated. The combined disinfectant effects of MH and LA contributed to the best *in vitro* inactivation performance of the combination treatment. Model fitting of the antibacterial kinetics revealed that the Weibull and reduced Baranyi models were superior to model the disinfectant kinetics of the three sanitising treatments of two *E. coli* strains, with higher R^2 and lower RMSE, SSE, and AIC values. Moreover, the results of protein leakage and

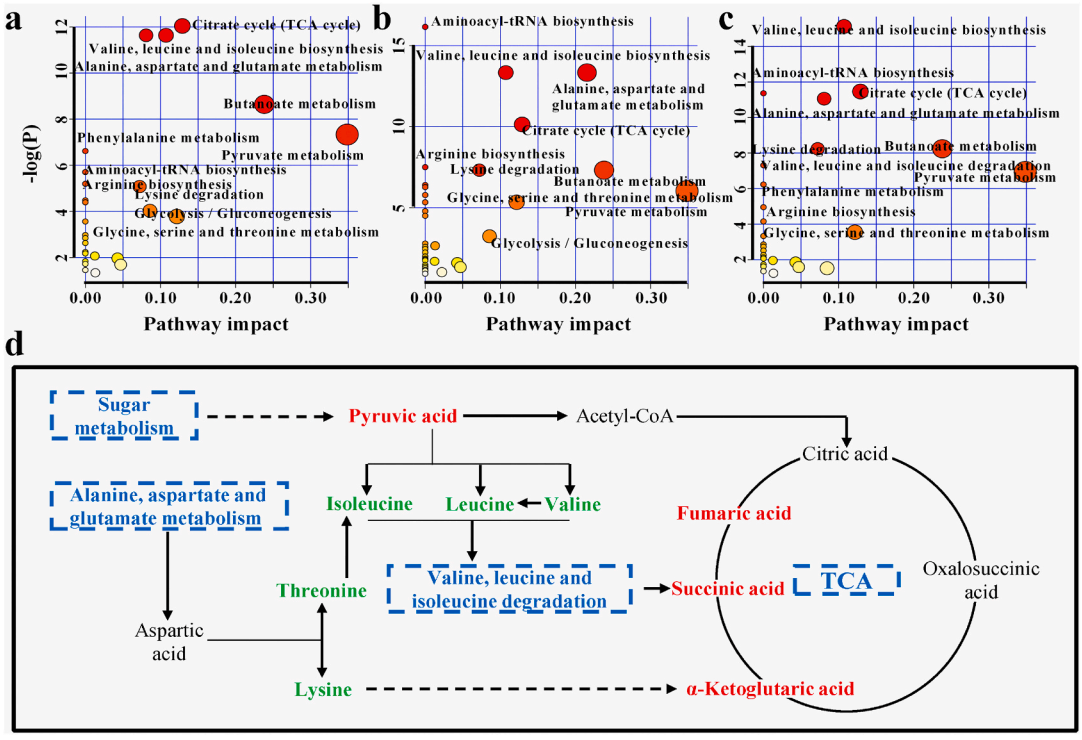

Fig. 7. Pathway analysis of pairwise groups I-II (a), I-III (b), I-IV (c); biochemical pathway of pathogenic *E. coli* O157:H7 under combination treatment (d). Note: I, control group; II, mild heat treatment; III, lactic acid treatment; IV, combination treatment.

AFM indicated that the inactivation of *E. coli* resulted from the outer membrane disruption MH treatment made the cell surface smoother and caused outer membrane damage. The membrane permeability was altered, accompanied by increased protein leakage. LA treatment almost destroyed the outer membrane and induced higher leakage of proteins. Furthermore, the disinfectant effect of LA treatment was enhanced by the combined use of MH. The *in vivo* growth curves in eight groups were recorded and the count reduction of *E. coli* during low temperature storage indicated the applicability of the inactivation treatments, especially the combined treatment. Model fitting showed that the Weibull model was applicable for the *in vitro* antibacterial effect and the *in vivo* growth kinetics. In addition, the physicochemical characteristics (colour, texture, and polyphenol content) of broccoli sprouts were not influenced by the processing strategies. Further metabolic study of PE showed that the energy supply and synthesis of related amino acid contributed to the acidic stress response. In conclusion, the combination of MH and LA could be a potential antibacterial method for organic sprouts.

CRediT authorship contribution statement

Lin Chen: Conceptualization, Methodology, Investigation, Software, Resources, Visualization, Writing – original draft. **Qin Liu:** Conceptualization, Methodology. **Xue Zhao:** Investigation, Software, Resources, Visualization. **Hongfei Zhang:** Software, Validation. **Xinyi Pang:** Software, Validation. **Hongshun Yang:** Conceptualization, Funding acquisition, Project administration, Supervision, Validation, Writing – review & editing.

Declaration of competing interest

We declare that we do not have any commercial or associative interest that represents a conflict of interest in connection with this manuscript. We have no financial and personal relationships with other people or organisations that can inappropriately influence our work.

Acknowledgements

This study was funded by Natural Science Foundation of Jiangsu Province (BK20181184), Applied Basic Research Project (Agricultural) Suzhou Science and Technology Planning Programme (SNG2020061), Singapore Ministry of Education Academic Research Fund Tier 1(R-160-000-A40-114), and an industry grant supported by Changzhou Qihui Management & Consulting Co., Ltd (R-160-000-A82-597).

Appendix A. Supplementary data

Supplementary data to this article can be found online at https://doi.org/10.1016/j.foodcont.2021.108577.

References

Abadias, M., Alegre, I., Oliveira, M., Altisent, R., & Viñas, I. (2012). Growth potential of *Escherichia coli* O157:H7 on fresh-cut fruits (melon and pineapple) and vegetables (carrot and escarole) stored under different conditions. *Food Control, 27*(1), 37–44.

Alakomi, H. L., Skyttä, E., Saarela, M., Mattila-Sandholm, T., Latva-Kala, K., & Helander, I. (2000). Lactic acid permeabilizes gram-negative bacteria by disrupting the outer membrane. *Applied and Environmental Microbiology, 66*(5), 2001–2005.

Baranyi, J., & Roberts, T. A. (1995). Mathematics of predictive food microbiology. *International Journal of Food Microbiology, 26*(2), 199–218.

Ben Braïek, O., & Smaoui, S. (2021). Chemistry, safety, and challenges of the use of organic acids and their derivative salts in meat preservation. *Journal of Food Quality*, 6653190, 2021.

Callejón, R. M., Rodríguez-Naranjo, M. I., Ubeda, C., Hornedo-Ortega, R., Garcia-Parrilla, M. C., & Troncoso, A. M. (2015). Reported foodborne outbreaks due to fresh produce in the United States and European union: Trends and causes. *Foodborne Pathogens and Disease, 12*(1), 32–38.

Chen, L., Tan, G. J. T., Pang, X., Yuan, W., Lai, S., & Yang, H. (2018). Energy regulated nutritive and antioxidant properties during the germination and sprouting of broccoli sprouts (*Brassica oleracea* var. *italica*). *Journal of Agricultural and Food Chemistry, 66*, 6975–6985.

Chen, L., Tan, J. T. G., Zhao, X., Yang, D., & Yang, H. (2019a). Energy regulated enzyme and non-enzyme-based antioxidant properties of harvested organic mung bean sprouts (*Vigna radiata*). *LWT – Food Science and Technology, 107*, 228–235.

Chen, L., Zhang, H., Liu, Q., Pang, X., Zhao, X., & Yang, H. (2019). Sanitising efficacy of lactic acid combined with low-concentration sodium hypochlorite on *Listeria innocua* in organic broccoli sprouts. *International Journal of Food Microbiology, 295*, 41–48.

Chen, L., Zhao, X., Wu, J. E., Liu, Q., Pang, X., & Yang, H. (2020). Metabolic characterisation of eight *Escherichia coli* strains including "Big Six" and acidic responses of selected strains revealed by NMR spectroscopy. *Food Microbiology, 88*, 103399.

Choi, S., Beuchat, L. R., Kim, H., & Ryu, J. H. (2016). Viability of sprout seeds as affected by treatment with aqueous chlorine dioxide and dry heat, and reduction of *Escherichia coli* O157:H7 and *Salmonella enterica* on pak choi seeds by sequential treatment with chlorine dioxide, drying, and dry heat. *Food Microbiology, 54*, 127–132.

Delaquis, P., Bach, S., & Dinu, L. D. (2007). Behavior of *Escherichia coli* O157:H7 in leafy vegetables. *Journal of Food Protection, 70*(8), 1966–1974.

Fan, X., Toivonen, P. M., Rajkowski, K. T., & Sokorai, K. J. (2003). Warm water treatment in combination with modified atmosphere packaging reduces undesirable effects of irradiation on the quality of fresh-cut iceberg lettuce. *Journal of Agricultural and Food Chemistry, 51*(5), 1231–1236.

Ferelli, A. M., & Micallef, S. A. (2019). *Food safety risks and issues associated with farming and handling practices for organic certified fresh produce. In Safety and Practice for Organic Food* (pp. 151–180). Academic Press.

Ghate, V., Kumar, A., Kim, M. J., Bang, W. S., Zhou, W., & Yuk, H. G. (2017). Effect of 460 nm light emitting diode illumination on survival of *Salmonella* spp. on fresh-cut pineapples at different irradiances and temperatures. *Journal of Food Engineering, 196*, 130–138.

Harvey, R. R., Zakhour, C. M., & Gould, L. H. (2016). Foodborne disease outbreaks associated with organic foods in the United States. *Journal of Food Protection, 79*(11), 1953–1958.

Huang, Y., & Chen, H. (2011). Effect of organic acids, hydrogen peroxide and mild heat on inactivation of *Escherichia coli* O157:H7 on baby spinach. *Food Control, 22*(8), 1178–1183.

Huang, L., Hwang, C. A., & Phillips, J. (2011). Evaluating the effect of temperature on microbial growth rate—the ratkowsky and a bělehrádek-type models. *Journal of Food Science, 76*(8), M547–M557.

Jozefczuk, S., Klie, S., Catchpole, G., Szymanski, J., Cuadros-Inostroza, A., Steinhauser, D., Selbig, J., & Willmitzer, L. (2010). Metabolomic and transcriptomic stress response of *Escherichia coli*. *Molecular Systems Biology, 6*, 364.

King, T., Lucchini, S., Hinton, J. C., & Gobius, K. (2010). Transcriptomic analysis of *Escherichia coli* O157:H7 and K-12 cultures exposed to inorganic and organic acids in stationary phase reveals acidulant-and strain-specific acid tolerance responses. *Applied and Environmental Microbiology, 76*, 6514–6528.

Koyama, K., Hokunan, H., Hasegawa, M., Kawamura, S., & Koseki, S. (2017). Estimation of the probability of bacterial population survival: Development of a probability model to describe the variability in time to inactivation of *Salmonella enterica*. *Food Microbiology, 68*, 121–128.

Lang, M. M., Ingham, B. H., & Ingham, S. C. (2000). Efficacy of novel organic acid and hypochlorite treatments for eliminating *Escherichia coli* O157:H7 from alfalfa seeds prior to sprouting. *International Journal of Food Microbiology, 58*(1–2), 73–82.

Liu, Q., Chen, L., Laserna, A. K. C., He, Y., Feng, X., & Yang, H. (2020). Synergistic action of electrolyzed water and mild heat for enhanced microbial inactivation of *Escherichia coli* O157:H7 revealed by metabolomics analysis. *Food Control, 110*, 107026.

Liu, Q., Tan, C. S. C., Yang, H., & Wang, S. (2017). Treatment with low-concentration acidic electrolysed water combined with mild heat to sanitise fresh organic broccoli (*Brassica oleracea*). *LWT-Food Science and Technology, 79*, 594–600.

Liu, Q., Wu, J. E., Lim, Z. Y., Lai, S., Lee, N., & Yang, H. (2018). Metabolite profiling of *Listeria innocua* for unravelling the inactivation mechanism of electrolysed water by nuclear magnetic resonance spectroscopy. *International Journal of Food Microbiology, 271*, 24–32.

Lu, G., Li, C., Liu, P., Cui, H., Yao, Y., & Zhang, Q. (2010). UV inactivation of microorganisms in beer by a novel thin-film apparatus. *Food Control, 21*(10), 1312–1317.

Lund, P., Tramonti, A., & De Biase, D. (2014). Coping with low pH: Molecular strategies in neutralophilic bacteria. *FEMS Microbiology Reviews, 38*(6), 1091–1125.

Luo, K., & Oh, D. H. (2016). Inactivation kinetics of *Listeria monocytogenes* and *Salmonella enterica* serovar *Typhimurium* on fresh-cut bell pepper treated with slightly acidic electrolyzed water combined with ultrasound and mild heat. *Food Microbiology, 53*, 165–171.

Mani-Lopez, E., García, H. S., & López-Malo, A. (2012). Organic acids as antimicrobials to control *Salmonella* in meat and poultry products. *Food Research International, 45*(2), 713–721.

Maresca, P., & Ferrari, G. (2017). Modeling of the microbial inactivation by high hydrostatic pressure freezing. *Food Control, 73*, 8–17.

McCollum, T. G., D'Aquino, S., & McDonald, R. E. (1993). Heat treatment inhibits mango chilling injury. *HortScience, 28*(3), 197–198.

Mukherjee, A., Speh, D., Dyck, E., & Diez-Gonzalez, F. (2004). Preharvest evaluation of coliforms, *Escherichia coli, Salmonella*, and *Escherichia coli* O157:H7 in organic and conventional produce grown by Minnesota farmers. *Journal of Food Protection, 67*(5), 894–900.

National Organic Program (NOP). (2011). *The use of chlorine materials in organic production and handling*. United States Department of Agriculture. NOP 5026 https://www.ams.usda.gov/sites/default/files/media/5026.pdf.

Nielsen, E. I., Cars, O., & Friberg, L. E. (2011). Predicting in vitro antibacterial efficacy across experimental designs with a semi-mechanistic PKPD model. *Antimicrobial Agents and Chemotherapy, 55*(4), 1571–1579.

Orth, J. D., Conrad, T. M., Na, J., Lerman, J. A., Nam, H., Feist, A. M., & Palsson, B.Ø. (2011). A comprehensive genome-scale reconstruction of *Escherichia coli* metabolism—2011. *Molecular Systems Biology, 7*, 535.

Pangloli, P., & Hung, Y. C. (2013). Reducing microbiological safety risk on blueberries through innovative washing technologies. *Food Control, 32*(2), 621–625.

Putker, F., Bos, M. P., & Tommassen, J. (2015). Transport of lipopolysaccharide to the Gram-negative bacterial cell surface. *FEMS Microbiology Reviews, 39*(6), 985–1002.

Scanlon, K. A., Tiwari, U., Cagney, C., Walsh, D., McDowell, D. A., & Duffy, G. (2015). Modelling the thermal inactivation of five *Campylobacteraceae* species. *Food Control, 47*, 135–140.

Sethi, S., Nayak, S. L., Joshi, A., & Sharma, R. R. (2020). *Sanitizers for fresh-cut fruits and vegetables. In fresh-cut fruits and vegetables* (pp. 99–119). Academic Press.

Sow, L. C., Tirtawinata, F., Yang, H., Shao, Q., & Wang, S. (2017). Carvacrol nanoemulsion combined with acid electrolysed water to inactivate bacteria, yeast in vitro and native microflora on shredded cabbages. *Food Control, 76*, 88–95.

Su, X., Wu, F., Zhang, Y., Yang, N., Chen, F., Jin, Z., & Xu, X. (2019). Effect of organic acids on bread quality improvement. *Food Chemistry, 278*, 267–275.

Tian, X., Yu, Q., Shao, L., Li, X., & Dai, R. (2018). Sublethal injury and recovery of *Escherichia coli* O157:H7 after ohmic heating. *Food Control, 94*, 85–92.

Townsend, A., Li, S., Mann, D. A., & Deng, X. (2020). A quasimetagenomics method for concerted detection and subtyping of *Salmonella enterica* and *E. coli* O157:H7 from romaine lettuce. *Food Microbiology, 92*, 103575.

Vandekinderen, I., Devlieghere, F., Van Camp, J., Kerkaert, B., Cucu, T., Ragaert, P., De Bruyne, J., & De Meulenaer, B. (2009). Effects of food composition on the inactivation of foodborne microorganisms by chlorine dioxide. *International Journal of Food Microbiology, 131*, 138–144.

Wang, C., Chang, T., Yang, H., & Cui, M. (2015). Antibacterial mechanism of lactic acid on physiological and morphological properties of *Salmonella Enteritidis, Escherichia coli* and *Listeria monocytogenes*. *Food Control, 47*, 231–236.

Wang, Y., Claeys, L., van der Ha, D., Verstraete, W., & Boon, N. (2010). Effects of chemically and electrochemically dosed chlorine on *Escherichia coli* and *Legionella beliardensis* assessed by flow cytometry. *Applied Microbiology and Biotechnology, 87*(1), 331–341.

Wang, C., Wang, S., Chang, T., Shi, L., Yang, H., Shao, Y., Feng, W., & Cui, M. (2013). Efficacy of lactic acid in reducing foodborne pathogens in minimally processed lotus sprouts. *Food Control, 30*(2), 721–726.

Yoon, J. H., & Lee, S. Y. (2018). Comparison of the effectiveness of decontaminating strategies for fresh fruits and vegetables and related limitations. *Critical Reviews in Food Science and Nutrition, 58*(18), 3189–3208.

Zhang, L., Alfano, J. R., & Becker, D. F. (2015). Proline metabolism increases *katG* expression and oxidative stress resistance in *Escherichia coli*. *Journal of Bacteriology, 197*, 431–440.

Zhang, Y., & Hu, Z. (2013). Combined treatment of *Pseudomonas aeruginosa* biofilms with bacteriophages and chlorine. *Biotechnology and Bioengineering, 110*(1), 286–295.

Zhao, X., Chen, L., Wongmaneepratip, W., He, Y., Zhao, L., & Yang, H. (2021). Effect of vacuum impregnated fish gelatin and grape seed extract on moisture state, microbiota composition, and quality of chilled seabass fillets. *Food Chemistry, 354*, 129581.

Zhao, L., Li, S., & Yang, H. (2021). Recent advances on research of electrolyzed water and its applications. *Current Opinion in Food Science*. https://doi.org/10.1016/j.cofs.2021.03.004